Available online at www.sciencedirect.com
ScienceDirect
Journal of the European Ceramic Society 31 (2011) 361–368
www.elsevier.com/locate/jeurceramsoc

Reactive infiltration processing (RIP) of ultra high temperature ceramics (UHTC) into porous C/C composite tubes

Daniel Doni Jayaseelan [a,*], Rafael Guimarães de Sá [a], Peter Brown [b], William E. Lee [a]

[a] *Centre for Advanced Structural Ceramics, Dept. of Materials, Imperial College London, SW7 2AZ, UK*
[b] *DSTL, Porton Down, Salisbury SP4 0JQ, UK*

Received 1 September 2009; received in revised form 4 October 2010; accepted 7 October 2010
Available online 11 November 2010

Abstract

A novel reactive infiltration processing (RIP) technique was employed to infiltrate porous carbon fibre reinforced carbon (C/C) composite hollow tubes with ultra high temperature ceramic (UHTC) particles such as ZrB_2. The C/C composite tubes had initial porosity of ~60% with a bimodal (10 μm and 100 μm) pore size distribution. A slurry with 40–50% ZrB_2 solid loading particles was used to infiltrate the C/C tubes. Our approach combines *in situ* ZrB_2 formation with coating of fine ZrB_2 particles on carbon fibre surfaces by a reactive processing method. A Zr and B containing diphasic gel was first prepared using inorganic–organic hybrid precursors of zirconium oxychloride ($ZrOCl_2{\cdot}8H_2O$), boric acid, and phenolic resin as sources of zirconia, boron oxide, and carbon, respectively. Then commercially available ZrB_2 powder was added to this diphasic gel and milled for 6 h. The resultant hybrid slurry was vacuum infiltrated into the porous hollow C/C tubes. The infiltrated tubes were dried and fired for 3 h at 1400 °C in flowing Ar atmosphere to form and coat ZrB_2 on the carbon fibres *in situ* by carbothermal reaction. Microstructural observation of infiltrated porous C/C composites revealed carbon fibres coating with fine nanosized (~100 nm) ZrB_2 particles infiltrated to a depth exceeding 2 mm. Ultra high temperature ablation testing for 60 s at 2190 °C suggested formation of ZrO_2 around the inner bore of the downstream surface.

Keywords: Reactive infiltration processing; Carbothermal reaction; C/C composites; ZrB_2; Sol–gel; Vacuum infiltration; Ablation resistance

1. Introduction

There is increasing demand for advanced materials with temperature capability of over 2000 °C for ultrahigh temperature and aerospace applications, such as rocket engines and thermal protection systems for space vehicles.[1–3] Although carbon fibre reinforced carbon matrix (C/C) composites have received much attention due to their excellent high-temperature strength, high thermal conductivity, low coefficient of thermal expansion (CTE), good thermal shock resistance and good ablation resistance,[4–8] their poor oxidation resistance above 500 °C restricts their high temperature applications. Various methods of providing oxidation resistance have been attempted including use of thin, prophylactic, coatings on the carbon fibres and particulate oxygen getters in the C/C matrix. Additives (such as B_4C, B_2O_3, SiC, and $MoSi_2$) doped into the C/C matrix have proven effective in improving oxidation resistance at low (<1000 °C) and medium temperatures (<1500 °C).[9–11] However, these oxygen inhibitors may not be effective in an ablative environment with high-pressure erosive gas flow and ultra-high temperatures (>2000 °C),[12] thus alternative oxidation inhibitors and other methods to provide oxidation protection for the C/C at ultra-high temperature are being sought.

Ceramic coatings can provide oxidation protection for C/C composites. For complete protection of C/C composites, at least three coatings are required: (i) on individual carbon fibres, (ii) on the filler material between C/C fibre composite and (iii) on the outer faces of the C/C composite. Key issues for such coatings are adherence, continuity and mechanical compatibility to resist spallation due to thermal expansion mismatch during extreme thermal excursions. Above all, the coating process should be simple so that coatings can be made reproducibly and reliably. A coating that is mechanically compatible with the substrate during extreme thermal heating should be used as the inner layer otherwise coating spallation and stress-induced cracking may result. Methods to promote adhesion of dense coatings and pre-

* Corresponding author.
E-mail address: d.j.daniel@imperial.ac.uk (D.D. Jayaseelan).

0955-2219/$ – see front matter.
doi:10.1016/j.jeurceramsoc.2010.10.013

vent delamination should consider materials that wet the C/C composite. Candidate materials for inner layers include reacted carbides and borate glasses.[13]

Ultra-high temperature ceramics (UHTCs) such as ZrB_2 and HfB_2 are candidate materials for use in extreme environments due to their high melting temperature and hardness, retained strength at high temperature and modest thermal expansion.[1,2,14–18] Introduction of UHTC-based ceramic particles into C/C composites improves the C/C oxidation resistance by gettering oxygen while the presence of carbon improves the UHTCs thermal shock resistance.

Processing methods for depositing coatings with fine grained microstructures include sputter deposition,[19] electroplating,[19] electron beam irradiation,[20] liquid precursor methods,[21,22] slurry coating,[23] pack cementation,[24] and chemical vapour deposition (CVD).[25,26] Each method has specific advantages for control of coating thickness and material composition enabling development of a wide range of coating microstructures and configurations. Corral et al.[13] developed UHTC coatings on C/C composites using inorganic–organic precursor solutions for infiltration and heat treatment at high temperatures (up to 2300 °C) to convert them to borides and carbides. Zou et al.[27] however, infiltrated Zr melt into porous C/C to form ZrC coatings.

In this paper, infiltration of ZrB_2 as an oxidation inhibitor into C/C composite tubes has been demonstrated using a conventional vacuum infiltration process. No attempt was made to perfect the processing route (e.g. by varying particle size and shape distributions, etc.) and this will the subject of future work. However, the novelty of the present infiltration-coating technique is that both ZrB_2 particles and an *in situ* formed ZrB_2 coating are utilised and the ZrB_2 coating not only forms a mechanical bond with the substrate but also a chemical bond arising from carbothermal reaction between Zr and B in the presence of C. This approach has the potential to give thorough C/C fibre coating with UHTC materials and hence to provide improved oxidation protection in severe environments.

2. Experimental details

2.1. Materials

Porous C/C tubes (Fig. 1) of 17.75 mm OD × 3.90 mm ID × 45 mm long were used in the present study for ZrB_2 infiltration. The porous C/C composite tubes had a total porosity of ~60% (measured using Archimedes method) and bimodal pore size distribution (determined using laser diffraction particle size analyser) with average pore sizes of 150 μm and 10 μm, respectively. ZrB_2 powder (d_{50} ~45 μm, 99% purity, Good Fellow, Huntingdon, UK) was used as the UHTC material. The as-received ZrB_2 powder was further dry-milled for 30 min in a "swing-mill" shatter box using a steel container coated with Teflon to reduce the average particle size to 5.11 ± 0.5 μm. Longer milling times (>30 min) did not result in significant reduction in the particle size. Particle size distribution analysis for milling times of 45 min and 60 min resulted in 50 wt.% of the materials being below 5.04 μm and 4.89 μm, respectively.

Fig. 1. Optical photograph of a porous C/C tube.

2.2. Infiltration process

2.2.1. ZrB_2 slurry

Wet slurry containing 50 wt.% solid loading of ZrB_2 was prepared for infiltration using ethanol. After wet ball-milling, the slurry was poured into a vacuum filtering-type glass flask and the porous C/C test samples were immersed inside the slurry. The air inside the flask was then evacuated using a vacuum pump with a pressure capacity of 10^{-3} Torr. As the air inside the flask was being extracted, the slurry begun to bubble signalling that trapped air was being extracted, thus enabling slurry infiltration into the pores. The vacuum pump was stopped about 30 min after the bubbling stopped. The sample was removed from the flask, dried for a day at room temperature and oven dried at 40 °C for 6 h before finally being dried for 24 h at 80 °C. Slow drying is necessary to avoid surface cracking of the coat.

2.2.2. "Gel-composite"

Zirconyl chloride octahydrate, $ZrOCl_2{\cdot}8H_2O$, 98% pure (Sigma Aldrich, Gillingham, UK), boric acid, H_3BO_3, 99.5% pure (Sigma Aldrich, Gillingham, UK) and solid phenolic resin, supplied by Schenectady Crios S/A (Sao Paulo, Brazil) under the brand name Novolaca, with a char yield of about 60 wt.%, were used as starting materials. The flowchart of the sol–gel preparation of ZrB_2 powder and infiltration process is shown in Fig. 2. 1 mole of $ZrOCl_2{\cdot}8H_2O$, 2 moles of H_3BO_3 and

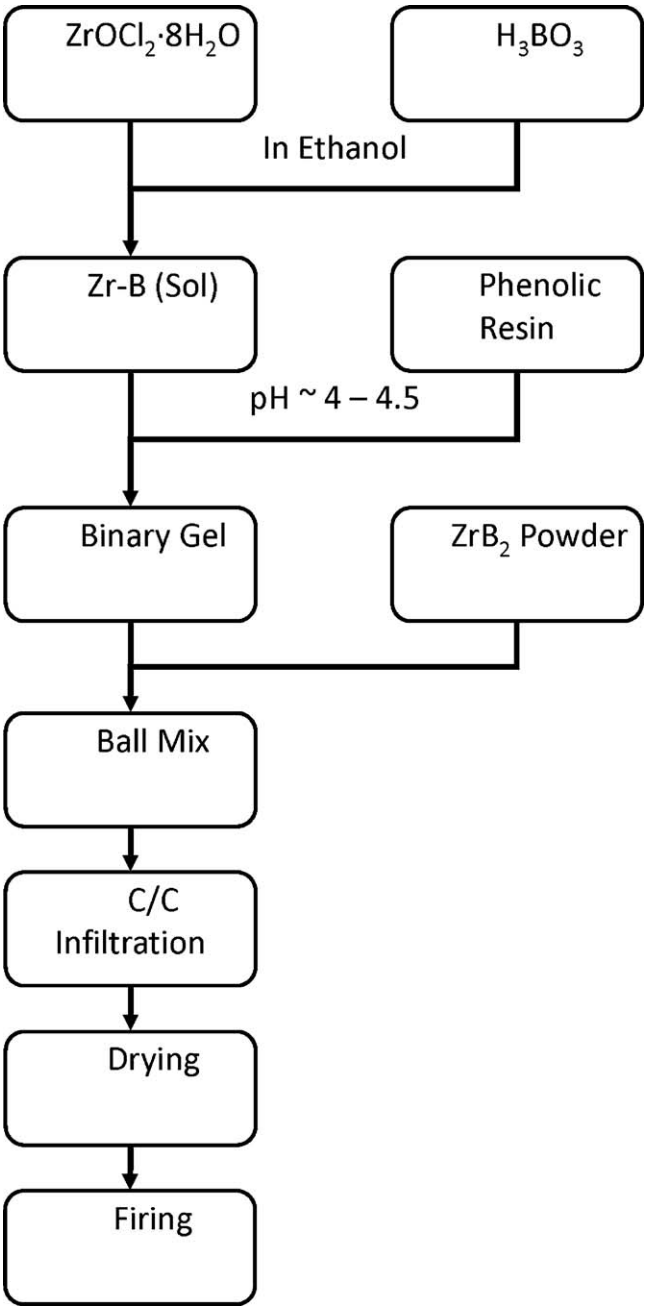

Fig. 2. Flow chart showing the coating process.

8.33 moles of phenolic resin were used to form stoichiometric ZrB_2. To promote molecular-level mixing between all the constituents of the reaction, they must be soluble in a solvent, which in this work was ethanol (98.5%, VWR, Lutterworth, UK). Initially, $ZrOCl_2 \cdot 8H_2O$, H_3BO_3 and phenolic resin were separately dissolved in the required amount of ethanol. The H_3BO_3 solution was then slowly added to the zirconyl chloride solution and mixed well under constant stirring. Later, the solution of phenolic resin was added to the above mixed solution and stirred continuously for 30 min. The pH of the mixed solution was adjusted between 4 and 4.5 under constant stirring using diluted ammonium hydroxide solution. The sol slowly became a Zr–B gel and the gel was ball mixed for 24 h using zirconia milling media. Commercial ZrB_2 powder was added to the precursor gel during ball mixing. The ball mixed gel containing ZrB_2 powder was used for vacuum infiltration. The dried infiltrated samples were then fired for 3 h at 1450 °C (heating/cooling rate = 5 °C/min) in flowing argon atmosphere to form ZrB_2 by the carbothermal reaction of ZrO_2 and B_2O_3 with carbon according to the following equation.

$$(1) ZrO_{2(s)} + B_2O_{3(s)} + 5C_{(s)} \rightarrow ZrB_{2(s)} + 5CO_{(g)}$$

The dried samples were weighed before and after infiltration to determine the amount of infiltrate loading.

2.3. Characterisation

Phase analysis of sol–gel derived precursor after heat treatment for 3 h at 1400 °C was carried out by X-ray diffraction (XRD) using a Philips PW7100 with using Cu Kα radiation. Infiltrated C/C tubes were sectioned and the microstructures of cross-sections of the infiltrated C/C tubes were analysed using a Field Emission Gun-Scanning Electron Microscope (FEG-SEM) LEO15 using both backscattered electron (BE) and secondary electron (SE) imaging modes along with Electron Dispersive X-Ray Spectroscopy (EDX) for chemical analysis.

2.4. Ultra high temperature ablation testing

Ultra high temperature ablation (UHTA) tests were carried out in a flowing air environment for the sol–gel derived ZrB_2 infiltrated and non-infiltrated porous C/C tubes for 80 s at temperatures of 2190 °C. The experimental set-up of UHTA testing is shown in Fig. 3. During the test, the specimen with a size of ∅17.75 mm OD × ∅3.12 mm ID × 45 mm long, mounted in a radiatively heated yttria stabilised zirconium oxide tube along which the heated gasses are passed. The distance between the nozzle tip of the gun and the top surface of the specimen was 10 mm. Optical images, Fig.11(c), of the samples before and after ablation tests were taken comparison.

3. Results and discussion

The Zr–B precursor gel used for infiltration was fired separately for 3 h at 1400 °C in flowing argon atmosphere. XRD (Fig. 4) confirms formation of ZrB_2. However, other phases, such as ZrC and *m*- and *t*-ZrO_2, were also observed. The presence of ZrC indicates boron deficiency during the carbothermal reaction most likely via B_2O_3 volatilisation above 1200 °C. Due to a scarcity of boron resulting from its volatilisation, the remaining ZrO_2 reacts with carbon to form ZrC. The presence of ZrO_2 indicates local oxygen contamination.

To compare qualitatively the proposed infiltration process, the porous C/C tubes were first infiltrated with ethanol-based slurry containing only commercial ZrB_2 powder. Multiple infiltrations were carried out to increase the extent of loading. The evolution of dry weight % (based on an untreated tube) of the porous C/C tubes was recorded as is shown in Fig. 5. Porous C/C tubes had nearly 40% weight gain after the 4th infiltration and clearly showed a trend of saturation from the 4th to the 5th infiltration

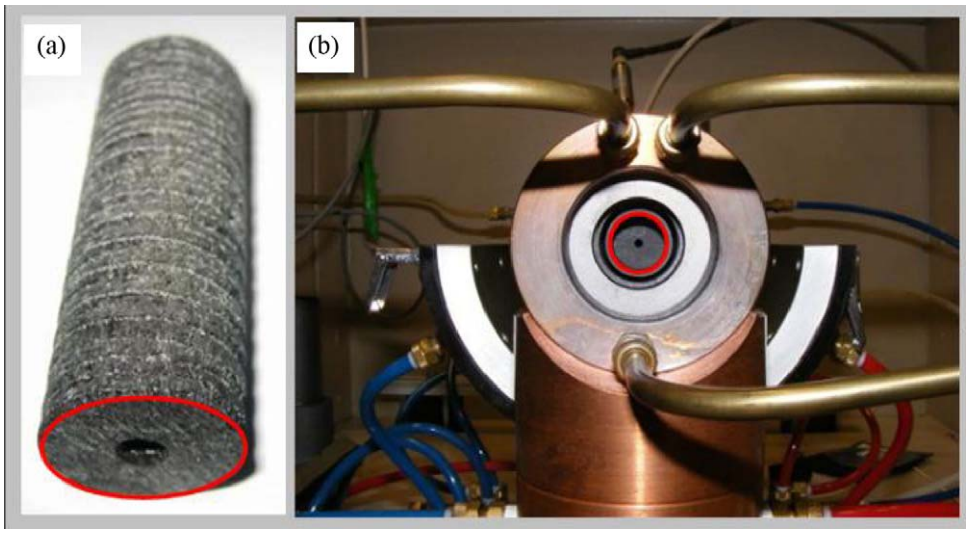

Fig. 3. Tubular C/C specimen (a) prior to ultra high temperature ablation (UHTA) testing and (b) located within the UHTA testing rig.

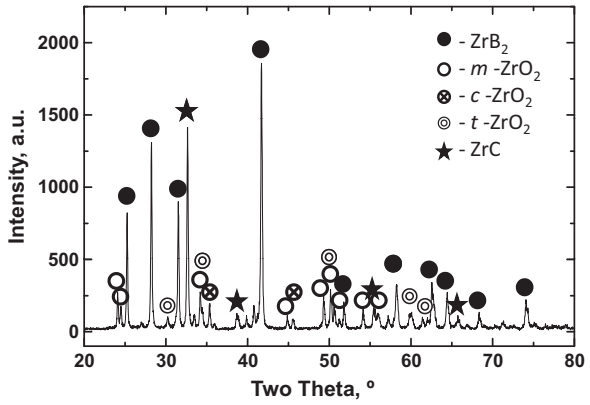

Fig. 4. XRD of sol–gel synthesised ZrB_2.

step and a decrease on the 6th infiltration step. Fig. 6 shows a BE image (a) and a SE image (b) of a C/C composite after the 4th infiltration step using an ethanol-based ZrB_2 slurry. The dark contrast regions in the BE image arise from lower atomic number elements (carbon) and the bright contrast regions are from phases containing heavier elements (Zr). Many ZrB_2 particles are present near the infiltration side surface, decreasing in number with infiltration depth. This is attributed to ZrB_2 particles at the front surface clogging the pores and preventing further particle ingress. Fig. 6(a) reveals ZrB_2 particles inside the porous C/C composite to a depth in excess of 2 mm. Fig. 6(b) illustrates the distribution of ZrB_2 particles in the voids between the C/C composite carbon fibres. Although the ZrB_2 particles infiltrated deep inside the porous body, they did not coat the carbon fibres but simply occurred as clusters between them.

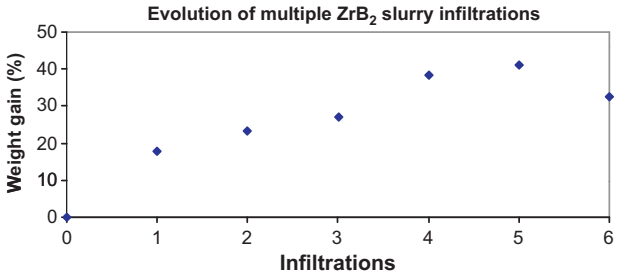

Fig. 5. Evolution (wt.% gain after drying based on a untreated tube) of multiple infiltrations by ethanol-based ZrB_2-slurry.

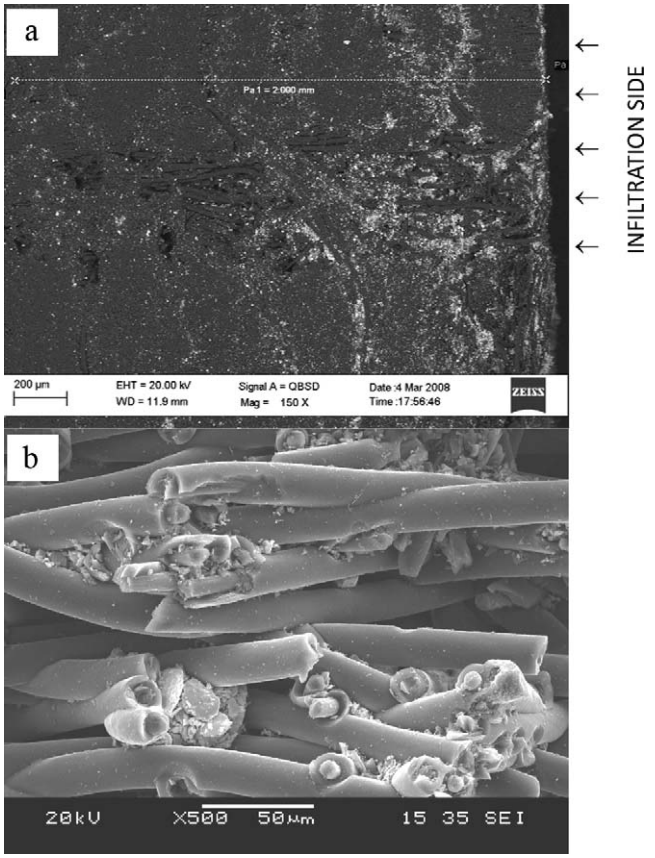

Fig. 6. (a) Backscattered electron (BE) cross-section image of a C/C composite after multiple infiltrations by an ethanol ZrB_2-based slurry. The dark regions are related to lower elements (carbon) and the bright regions to heavier elements (Zr) and (b). ZrB_2 particles distributed along the carbon fibres.

To overcome the lack of bonding between the fibres and ZrB_2 particles, sol–gel coating by infiltration of the ZrB_2 precursor gel was attempted. However, samples of gel penetrated porous C/C composite only gained 2.02% by weight, indicating little ZrB_2 loading inside the sample after a single infiltration. Microstructural observation revealed that only a thin layer of ZrB_2 particles (few μm) coated the surface of the carbon fibres after a single infiltration step. There was no evidence of ZrB_2 particles inside the C/C porous body, between the fibres. This was caused by the characteristically low yield (20–30 wt.%) of the sol–gel route.

To improve infiltration quality and quantity, a "gel-composite" infiltration process (Fig. 2) was carried out. The composite slurry containing Zr–B gel and commercial ZrB_2 powder (with 50 wt.% solid loading in total) was used for infiltration. Fig. 7 shows a BE image of a cross section of a "gel-composite" infiltrated C/C composite after thermal treatment for 3 h at 1400 °C. Although the C/C composite sample was carefully sectioned using sharp blades, some bright contrast particles were dislodged during this process. It was observed that lighter contrast regions of particles coated the carbon fibres in a patchy manner. The arrows show the infiltration sides. EDX analysis revealed that brighter agglomerates are infiltrated ZrB_2 particles, which are clearly seen at a depth of >3 mm. About 30 wt.% of ZrB_2 particles infiltrated the porous C/C composites with little evidence of pore clogging.

Fig. 8(a)–(d) shows the microstructure of a "gel-composite" infiltrated C/C composite at different magnifications. Individual carbon fibres after "gel-composite" infiltration can be seen in

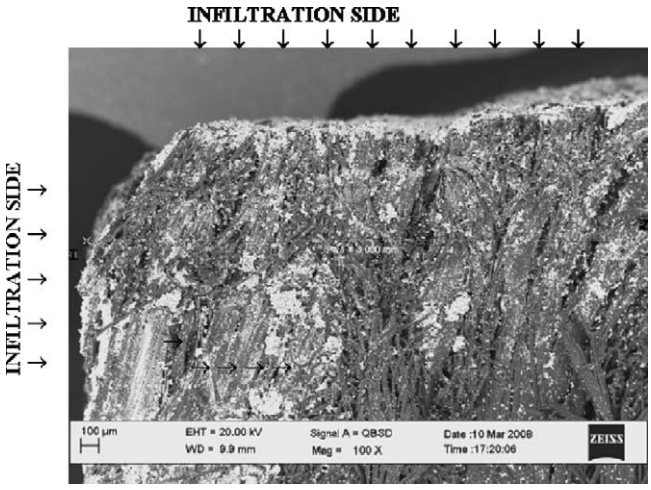

Fig. 7. BE image of a C/C composite after composite sol–gel infiltration. The bright contrast regions over the carbon fibres are ZrB_2 coatings.

Fig. 8(a). Higher magnification of these individual carbon fibres in Fig. 8(b) and (c) show that carbon fibres were coated in patches with fine (~100 nm) particles. No visible cracks occurred in the coatings and the coatings were porous in nature. Temperatures above 2000 °C are likely to be necessary to obtain denser coatings. Magnified images, Fig. 8(c) and (d), revealed that the fibre surface was rough. It became evident from Fig. 8(c) that the carbon fibre had chemically reacted with the particles. The interesting feature is that the ZrB_2 particles were not simply

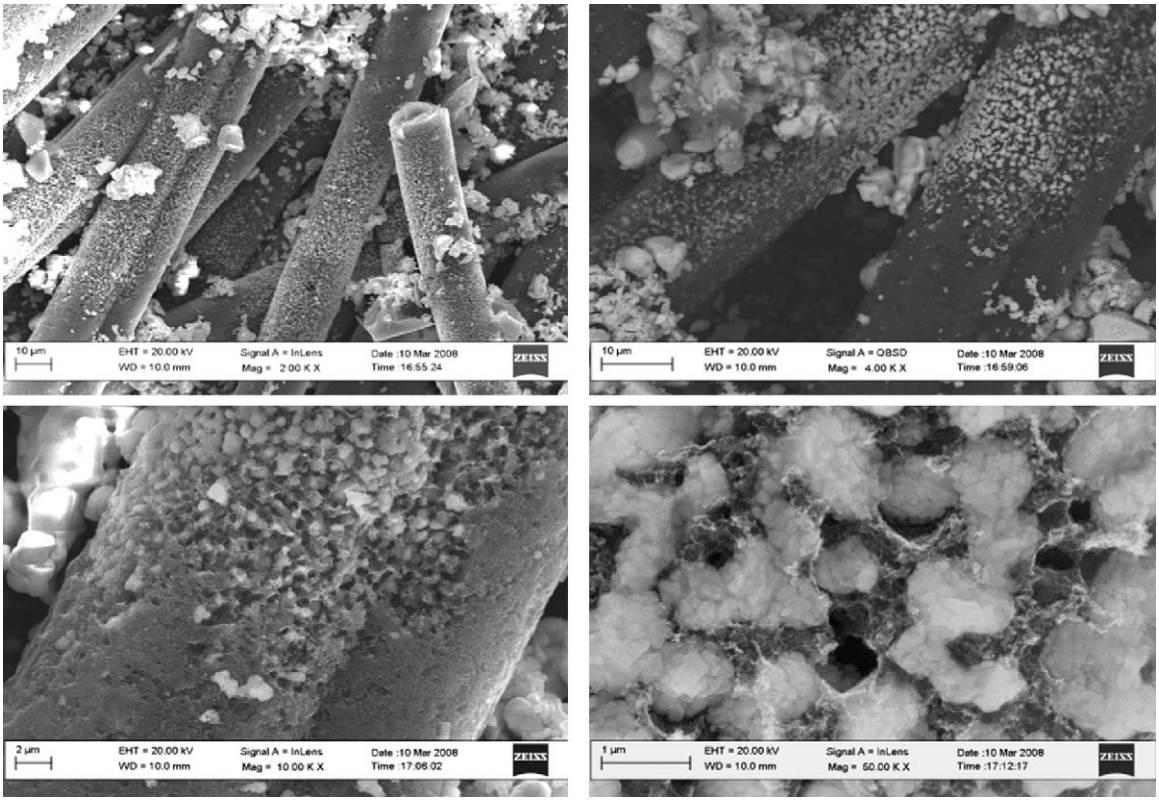

Fig. 8. (a–c) Images of sol–gel coatings at different magnifications showing that ZrB_2 is chemically bonded to the fibre's carbon, which reacted carbothermally with it and (d) shows the nano-sized ZrB particles agglomerated together on carbon fibre.

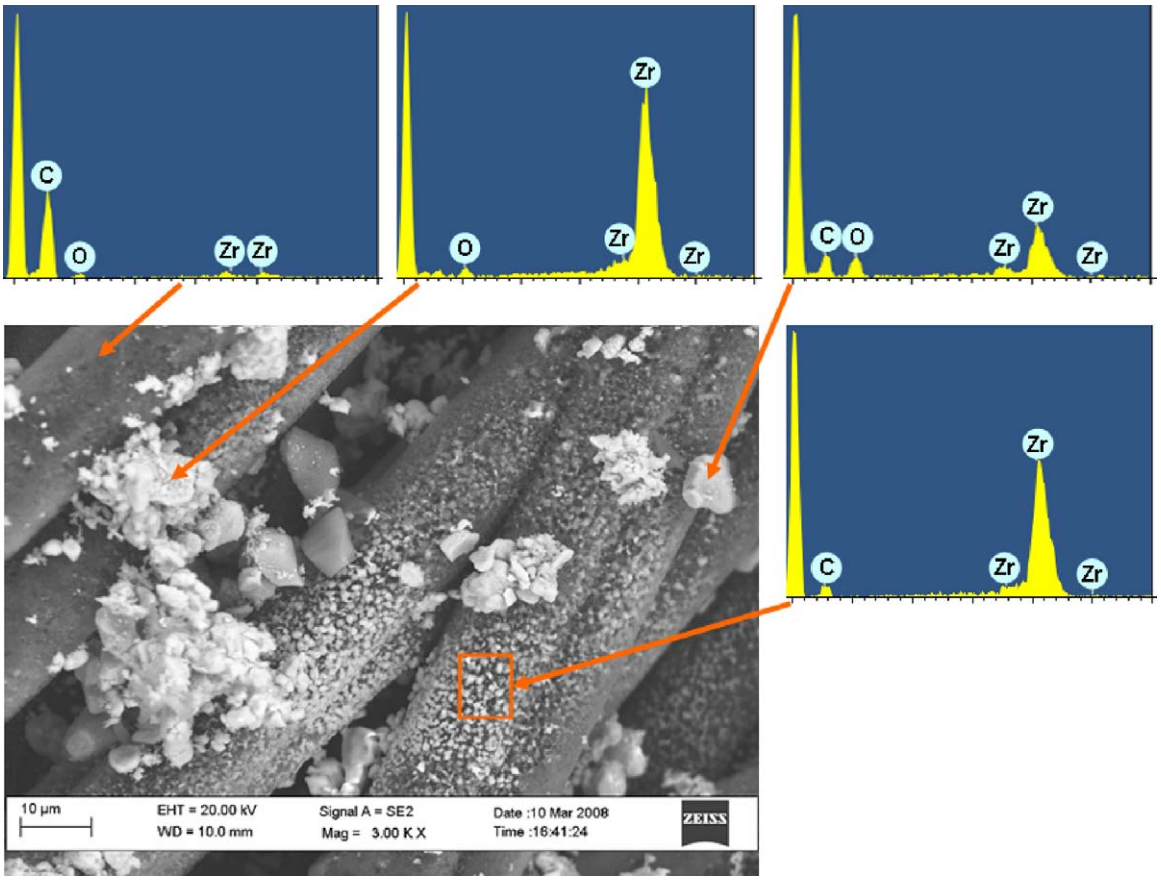

Fig. 9. EDX analysis of the composite slurry infiltration after thermal treatment.

physically adhered to the fibre surfaces, but, due to participation of the carbon from the fibre surface in the carbothermal reaction on firing, they were truly chemically bonded to the fibre surfaces. The high magnification SE image in Fig. 8(d) shows in detail the fine (<100 nm) structure of the chemically bonded ZrB_2 particles. These nanosized ZrB_2 particles were formed by the in *situ* carbothermal reaction between Zr and B in presence of C contained in the precursor gel and the fibre surface.

Fig. 9 shows EDX analysis of the infiltrated porous C/C composite using the "gel-composite" slurry. In all regions, it reveals the presence of Zr. EDX analysis on the bright contrast particles reveals mainly Zr and a trace of O. Boron could not be detected using the FEG-SEM LEO15 EDX system. This is strong evidence for *in situ* formation and coating of ZrB_2 particles on the carbon fibres. In some places, oxygen is arising from ZrO_2 formed during *in situ* formation of ZrB_2. The presence of carbon in the EDX spectrum could be either from the carbon fibre or from ZrC formation.

A schematic representation of the formation of ZrB_2 coating is shown in Fig. 10. After infiltration of the "gel-composite" into the porous C/C composites, they were fired for 3 h at 1400 °C in argon atmosphere. On firing, ZrO_2 reacts with gel-containing B_2O_3 via carbon from the fibres by a carbothermic reaction. Thus the fibre surfaces participate in the reaction process to form a thin (100 nm) coating on their surfaces (light grey in Fig. 10). This is a reactive infiltration process (RIP) for coating of ZrB_2 on the carbon fibre surfaces. Once a chemically bonded coating

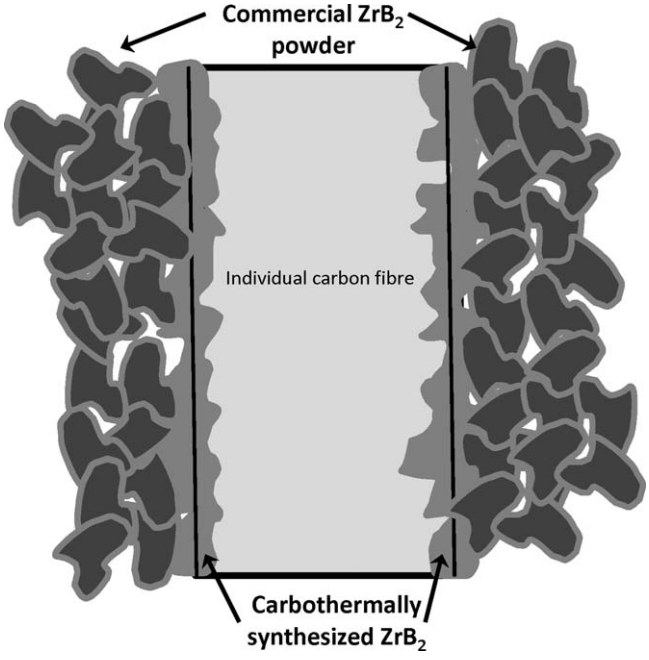

Fig. 10. Schematic of the formation of ZrB_2 on a carbon fibre.

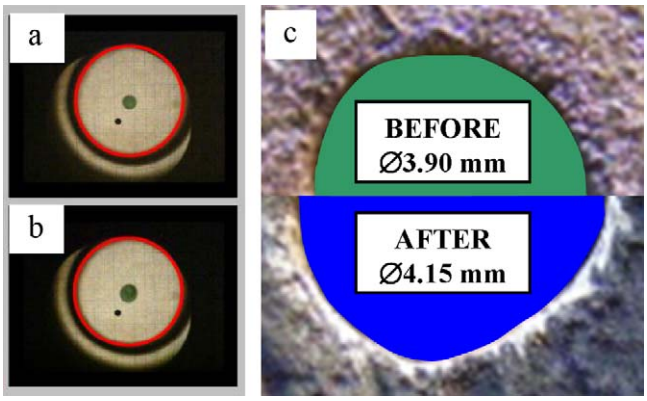

Fig. 11. Optical images of tubular C/C specimen in the UHTA test rig (a) prior to and (b) after testing. (c) Compares the bore of the sol–gel infiltrated ZrB^2 C/C tube before and after testing revealing formation of a white phase in the bore on UHTA believed to be ZrO_2.

is formed on the surface, it acts as a platform for accommodation of commercial ZrB_2 particles (dark grey in Fig. 10). Thus, infiltrating the slurry of combined gel and powder gives a distinct advantage. The gel helps to coat the C/C and the ZrB_2 coating acts as an interphase layer between the infiltrated commercial ZrB_2 particles and the carbon fibres.

Optical images of the response of porous C/C tubes before and after an ablation test for 60 s at 2500 °C are shown in Fig. 11(a) and (b), respectively. An increase in the inner diameter of the C/C tube has been observed with increase in ablation time suggesting erosion of the tube. The ablation performance of the tube does not therefore appear to have been improved. Higher magnification examination of the bore of the ZrB_2 sol–gel infiltrated C/C tube after ablation testing (Fig. 11(c)) reveals a white contrast phase surrounding the bore suggesting formation of ZrO_2. Since the erosion/corrosion mechanism associated with the ablation test is not fully understood detailed discussion of it is beyond the scope of this paper which is focused on the processing method of UHTC and C/C composites. However, it is likely that oxidation of the ZrB_2 to ZrO_2 is helping to protect the C/C by gettering oxygen as is well-established when using similar (e.g. B_4C) antioxidants in C-containing refractory bricks.[28] Improvements to the infiltration process, perhaps using smaller ZrB_2 particles or greater loadings and more infiltrations, would likely confer better oxidation resistance potentially by formation of a fully dense and protective ZrO_2 layer on the C/C. Follow on work in this programme[29] has established improved processing parameters to achieve this.

4. Conclusions

Porous C/C composite tubes were successfully infiltrated with ZrB_2 particles to a maximum depth of more than 3 mm. Three different types of slurry were used for the powder infiltration. The first type used was a non-aqueous based ZrB_2 slurry. An infiltration depth of over 2 mm was achieved using this powder slurry. However, pore clogging tends to persist at the infiltration side and the powder distribution density tends to decrease with infiltration depth. The second type of slurry used was a ZrB_2 gel. *In situ* formation and coating of ZrB_2 particles were obtained by this method. Although fine (<100 nm) ZrB_2 particles were well coated on the carbon fibre, the number of ZrB_2 particles inside the pores was low. The third type of slurry used was the "gel-composite" slurry containing ZrB_2 gel and commercial ZrB_2 powder. Nearly 30 wt.% of ZrB_2 particles was infiltrated into porous C/C to a depth of over 3 mm. No pore clogging was observed. Thin nanosized ZrB_2 coatings on the carbon fibres act as an interphase layer between the infiltrated commercial ZrB_2 particles and the carbon fibre. As the formation of ZrB_2 on carbon fibre arises from reaction bonding, it has the potential to improve the oxidation and ablation resistance of the C/C composite significantly.

Acknowledgments

Author DDJ thanks the Defence Science and Technology (Dstl) for providing the financial support for this work under contract number DSTLX-1000015413.

References

1. Savino R. Aerothermodynamic study of UHTC-based thermal protection systems. *Aerospace Science and Technology* 2005;**9**(2):151–60.
2. Chamberlain AL, Fahrenholtz WG, Hilmas GE, Ellerby DT. Characterization of zirconium diboride for thermal protection systems. *Key Engineering Materials* 2004;**Euro Ceramics VIII**:493–6.
3. Yang Y, Yang J, Fang D. Research progress on thermal protection materials and structures of hypersonic vehicles. *Applied Mathematics and Mechanics* 2008;**29**(1):51–60.
4. Luo RY, Liu T, Li JS, Zhang HB, Chen ZJ, Tian GL. Thermophysical properties of carbon/carbon composites and physical mechanism of thermal expansion and thermal conductivity. *Carbon* 2004;**42**(14):2887–95.
5. Han JC, He XD, Du SY. Oxidation and ablation of 3D carbon–carbon composite at up to 3000 °C. *Carbon* 1995;**33**(4):473–8.
6. Fitzer E. The future of carbon–carbon composites. *Carbon* 1987;**25**(2):163–90.
7. Awasthi E, Wood JL. C/C composite materials for aircraft brakes. *Advanced Ceramic Materials* 1987;**3**(5):449–51.
8. Blanco C, Casal E, Granda M, Menéndez R. Influence of fibre-matrix interface on the fracture behaviour of carbon-carbon composites. *Journal of the European Ceramic Society* 2003;**23**(15):2857–66.
9. Park SJ, Seo MK, Lee DR. Studies on the mechanical and mechanical interfacial properties of carbon–carbon composites impregnated with an oxidation inhibitor. *Carbon* 2003;**41**(15):2991–3002.
10. Luo RY, Yang Z, Li LF. Effect of additives on mechanical properties of oxidation-resistant carbon/carbon composite fabricated by rapid CVD method. *Carbon* 2000;**38**(15):2109–15.
11. Sogabe T, Okada O, Kuroda K, Inagaki M. Improvement in properties and air oxidation resistance of carbon materials by boron oxide impregnation. *Carbon* 1997;**35**(1):67–72.
12. Tripp WC, Graham HC. Thermogravimetric study of oxidation of ZrB_2 in temperature range of 800 °C to 1500 °C. *Journal of the Electrochemical Society* 1971;**118**(7):1195.
13. Corral EL, Loehman RE. Ultra-high-temperature ceramic coatings for oxidation protection of carbon–carbon composites. *Journal of the American Ceramic Society* 2008;**91**(5):1495–502.
14. Wuchina E, Opila E, Fahrenholtz WG, Talmy IG. UHTCs: ultra-high temperature ceramic materials for extreme environment applications. *Interface* 2007;**16**(4):30–6.
15. Monteverde F, Fabbriche DD, Bellosi A. Zirconium diboride-based composites. *Euro Ceramics* 2002;**Vii**(Pt 1–3):961–4.
16. Monteverde F, Bellosi A. The resistance to oxidation of an HfB_2-SiC composite. *Journal of the European Ceramic Society* 2005;**25**(7):1025–31.

17. Monteverde F. Processing and properties of ultra-high temperature ceramics for space applications. *Materials Science & Engineering A Structural Materials* 2008;**485**(1–2):415–21.
18. Chamberlain AL, Fahrenholtz WG, Hilmas GE, Ellerby DT. High-strength zirconium diboride-based ceramics. *Journal of the American Ceramic Society* 2004;**87**(6):1170–2.
19. Sheehan JE. High-temperature coatings on carbon fibers and carbon–carbon composites. In: Buckley JD, Edie DD, editors. *Carbon–carbon materials and composites*. Norwich: William Andrew Inc.; 1993. p. 223–66.
20. Alvey MD, George PM. $ZrPt_3$ as a high-temperature, reflective, oxidation-resistant coating for carbon–carbon composites. *Carbon* 1991;**29**(415):523–30.
21. Jensen JA, Gozum JE, Pollina DM, Girolami GS. Titanium, zirconium, and hafnium tetrahydroborates as "tailored" CVD precursors for metal diboride thin films. *Journal of the American Ceramic Society* 1988;**110**(5):1643–4.
22. Yongjie Y, Zhengren H, Shaoming D, Dongliang J. New route to synthesize ultra-fine zirconium diboride powders using inorganic–organic hybrid precursors. *Journal of the American Ceramic Society* 2006;**89**(11): 3585–8.
23. McKee DW. Oxidation behavior and protection of carbon–carbon composites. *Carbon* 1987;**25**(4):551–7.
24. Fu QG, Li HJ, Shi XH, Li KZ, Sun GD. Silicon carbide coatings to protect carbon/carbon composites against oxidation. *Scripta Materialia* 2005;**52**(9):923–7.
25. Chown J, Deacon RF, Singer N, White AES. Refractory coatings on graphite. In: Popper P, editor. *Special ceramics*. Academic Press; 1963. p. 1–81.
26. Cermignani W, Paulson T, Onneby C. Synthesis and characterization of boron-doped carbons. *Carbon* 1995;**33**(4):367–74.
27. Zou L, Wali N, Yang J-M, Bansal NP. Microstructural development of a Cf/ZrC composite manufactured by reactive melt infiltration. *Journal of the European Ceramic Society* 2008;**30**(6):1527–35.
28. Lee WE, Moore RE. Evolution of *in-situ* refractories in the 20th century. *Journal of the American Ceramic Society* 1998;**81**(6):1385–410.
29. Paul A.J. and Binner J, unpublished work.